Visualizing Halogen Bonds in Planar Supramolecular Systems
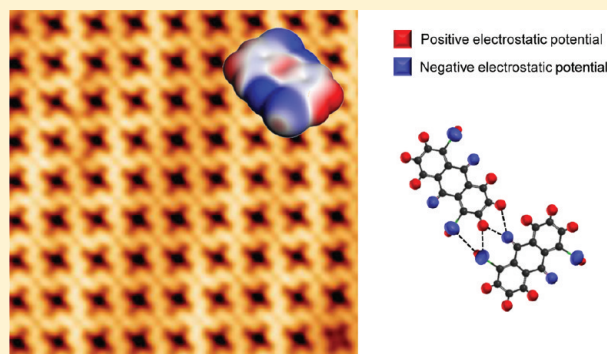
Jong Keon Yoon,[†] Won-joon Son,[‡] Kyung-Hoon Chung,[†] Howon Kim,[†] Seungwu Han,[‡] and Se-Jong Kahng*,[†]

[†]Department of Physics, Korea University, 1-5 Anam-dong, Seongbuk-gu, 136-713, Seoul, South Korea
[‡]Department of Materials Science and Engineering, Seoul National University, Seoul 151-744, South Korea

Ⓢ *Supporting Information*

ABSTRACT: Supramolecular interactions were studied in two planar model systems, 1,5- and 2,6-dibromoanthraquinones, prepared on Au(111) using scanning tunneling microscopy. In both systems, we found rigid triangular structures that consisted of simultaneous halogen bonds and hydrogen bonds, as reported in protein—ligand complexes. We proposed molecular models that were well reproduced by first-principle studies and could be explained by halogen and hydrogen bonds. The distances, angles, and, strengths of the intermolecular bonds were measured in the observed structures, and showed good agreement with existing bulk data.

1. INTRODUCTION

Covalently bonded halogen-ligands possess unusual charge distributions, attracting nucleophilic molecular ligands to form halogen bonds.[1−4] Due to their favorable lipophilicity, halogen ligands are used in a substantial portion of antibiotic inhibitors and drug candidates to enhance membrane penetration.[5−10] In these large molecular biosystems, halogen bonds compete with coexisting hydrogen bonds to determine the functional conformations of secondary and higher-order structures of macromolecules.[11−13] In protein—ligand complexes, molecular structures are often compromised by having simultaneous halogen and hydrogen bonds (O···Br and H···O, respectively) that make triangular structures.[12] Similar triangular structures consisting of different halogen and hydrogen bonds (Br···Br and H···Br, respectively), were also recurrently found in the crystals of small molecular systems, implying that the triangular structures provide an efficient way to form rigid structures using halogen and hydrogen bonds irrespective of molecular dimensions.[14−16] In such small molecular model systems, the interplay between halogen and hydrogen bonds has been exploited in the spontaneous construction of self-assembled molecular arrays and cocrystals.[17−22]

Studies of both large and small molecular systems have been based on the experimental methods of X-ray diffraction, nuclear magnetic resonance, infrared spectroscopy, solution calorimetry, and so forth.[11,14−21] The results of these studies consistently suggest that halogen and hydrogen bonds either compete or cooperate, with their similar bond strength and dissimilar directionality, in constructing stable intermolecular structures (e.g., triangular structures).[14−21] However, the experimental methods

follow an ensemble-averaging approach. It was not possible to extract local and individual molecular information, which is a crucial part of supramolecular study, for further applications.

In this work, we directly visualized the molecular configurations and the role of halogen and hydrogen bonds in planar model systems prepared on Au(111) using scanning tunneling microscopy (STM). Supramolecular structures of two geometrical isomers, 1,5- and 2,6-dibromoanthraquinones (DBAQ), were compared to unravel different triangular structures having Br···Br or O···Br halogen bonds. With the help of first-principle studies, we considered the distances, angular structures, and strengths of the observed halogen and hydrogen bonds.
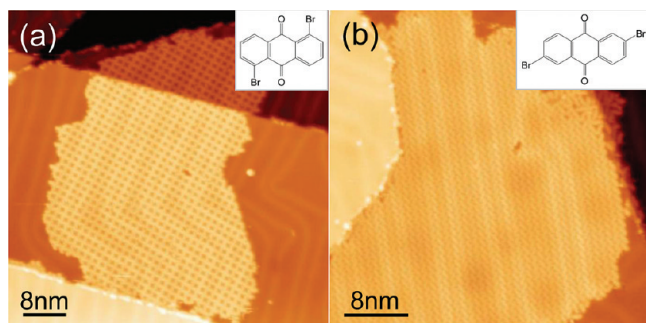
2. EXPERIMENTAL SECTION

All STM experiments were performed using a home-built STM housed in an Ultra High Vacuum chamber with a base pressure below 7×10^{-11} Torr. The Au(111) surface was prepared from a thin film (200-nm thick) of Au on mica that was exposed to several cycles of Ar-ion sputtering and annealing at 800 K over the course of 1 h. The surface cleanliness of the Au(111) was checked by observing typical herringbone structures on the terraces in the STM images. Commercially available 1,5- and 2,6-DBAQ (Tokyo Chemical Industry) was outgassed in a vacuum for several hours and then deposited on the Au(111) at submonolayer coverage by thermal evaporation using an alumina-coated evaporator. STM images were obtained at constant-current

Figure 1. Typical STM images of the two-dimensional supramolecular structures of (a) 1,5- and (b) 2,6- dibromianthraquinone (DBAQ) molecules. Their chemical structures are drawn in the insets. Sizes of STM images: (a) 60×60 nm^2 and (b) 40×40 nm^2. Tunneling current: $I_T = 0.1$ nA. Sample voltage: $V_S = -2.0$ V.
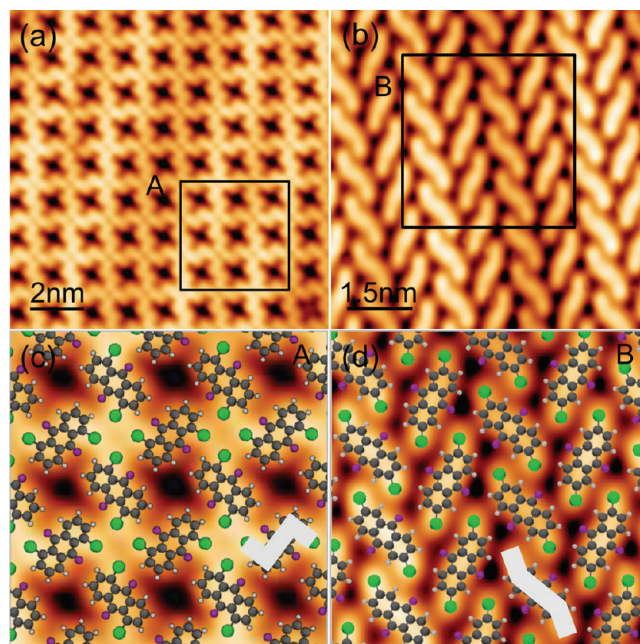
mode with a Pt/Rh tip while keeping the sample temperature at 80 K.

3. THEORETICAL CALCULATIONS

We performed first-principles density-functional calculations with the VASP code.[23,24] Interaction between ions and electrons is approximated by the projector-augmented wave (PAW) potential.[25] The generalized gradient approximation (GGA) with the Perdew—Burke—Ernzerhof (PBE) functional is used to describe the exchange correlations between electrons.[26] The energy cutoff for the plane wave basis is set to 600 eV. The functional dependence was checked with the hybrid functional method based on the B3LYP scheme.[27−30] The lattice parameters and molecular geometries were very similar to those by PBE functional. To describe nonbonding interactions between the molecules, especially of van der Waals type, an empirical correction scheme proposed by Grimme et al. was adopted.[31] The energy and electrostatic potential for the isolated molecules are obtained by using $35 \times 35 \times 20$ Å^3 supercell. A simulation cell containing two DBAQ molecules was adopted to describe the periodic structure. The height of the simulation box perpendicular to the molecule plane is fixed to 10 Å, while the lateral cell parameters are optimized such that the residual stress is reduced under 1 kbar.

4. RESULTS AND DISCUSSION

The chemical structures of 1,5- and 2,6 -DBAQ molecules are shown in the insets of Figure 1, parts (a) and (b). Since the molecules have six H, two O, and two Br atoms, it is expected that halogen and/or hydrogen bonds will form between two neighboring molecules. When 1,5- and 2,6-DBAQ molecules are deposited on Au(111), they diffuse to form molecular islands at 200 K. Figure 1, parts (a) and (b), shows STM images obtained after DBAQ was deposited to the substrate. We observed well-ordered supramolecular islands that preserved the herringbone corrugations of Au(111). In 1,5-DBAQ, a square-like structure formed, whereas in 2,6-DBAQ a chevron-like structure formed, as shown in the enlarged images of Figure 2, parts (a) and (b). In order to identify individual molecules in the supramolecular structures, we measured STM images at various energy levels between −1.5 eV and +1.5 eV near the Fermi level (see Figures S1 and S2 in Supporting Information), and observed that they had modest variations in energy levels. Both individual
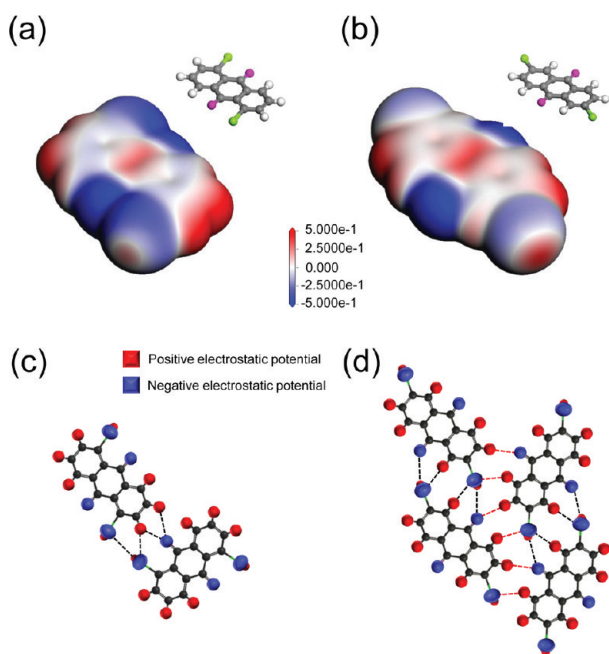

Figure 2. Higher resolution (compared to Figure 1) STM images of (a) 1,5- and (b) 2,6- DBAQ molecules. Molecular models of (c) 1,5- and (d) 2,6- DBAQ are superimposed over the STM images that are magnified from the squared regions in (a) and (b), respectively. Individual molecules are identified by crank shapes in gray. Sizes of STM images: (a) 12×12 nm^2 and (b) 7×7 nm^2. Tunneling current: $I_T = 0.1$ nA. Sample voltage: (a) $V_S = -1.5$ V and (b) $V_S = +0.5$ V.

molecules showed crank-like shapes. On the basis of this, we propose models for supramolecular structures, which are shown overlaid on STM images in Figure 2, parts (c) and (d). Both molecules possess prochirality. The 1,5-DBAQ structure consists of only one-type of prochiral molecules, whereas the 2,6-DBAQ structure comprises of two-different prochiral molecules.[32,33]

To understand the mechanisms of intermolecular interactions, we calculated the spatial distributions of electrostatic potentials for isolated 1,5-DBAQ and 2,6-DBAQ molecules using first-principles methods based on the generalized gradient approximation (GGA).[26] Figure 3, parts (a) and (b), shows the electrostatic potential mapped on the isosurfaces of 0.003 e/Bohr^3. The positive and negative potentials are color-coded in red and blue, respectively. H atoms (in red) have positive electrostatic potential, while O atoms (in blue) have negative electrostatic potential. These results can be understood by the large electronegativity differences between them (H: 2.20, O: 3.44). Br atoms have both red and blue regions with cylindrical symmetry about the axis of the covalent bond. These kinds of potential distributions form, when Cl, Br, and I atoms are covalently bonded to other atoms such as C, N, and halogen.[1−4] Although the positive potential region cannot be understood by a simple electronegativity consideration (Br: 2.96), this unique potential distribution is the result of interplay between the Schrödinger equation and the Poisson equation, and is the physical origin of halogen bonds.[1−4]

Intermolecular interactions in the 1,5-DBAQ (2,6-DBAQ) structures can be explained by considering two (four) nearest neighbor molecules. In Figure 3, parts (c) and (d), two and four molecules are drawn, respectively. Potential configurations around the H, O, and Br atoms are expressed with the simplified versions of Figures 3(a) and (b). Intermolecular interactions between the two 1,5-DBAQ molecules are quite clear. There are
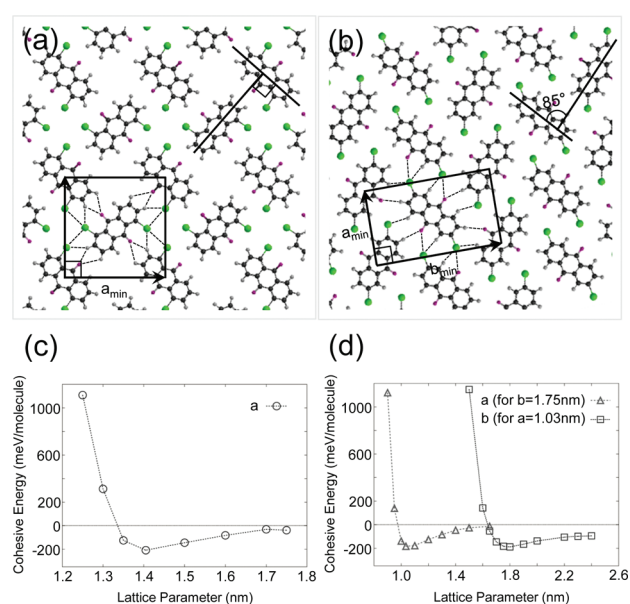
Figure 3. Calculated molecular electrostatic potential distributions (in volts) of (a) 1,5- and (b) 2,6- DBAQ molecules at isodensity surfaces, shown in red (positive) and blue (negative). Schematic illustrations for (c) two nearest neighbor 1,5- and (d) four nearest neighbor 2,6-DBAQ molecules with simplified electrostatic potential distributions around H, O, and Br atoms. The dotted lines indicate possible intermolecular bonds.
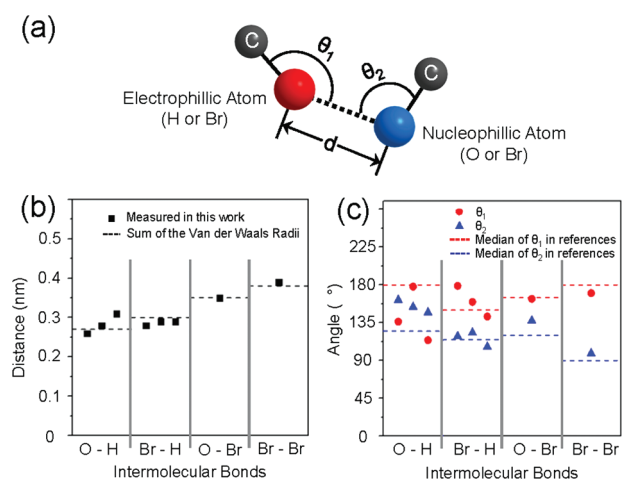

Figure 4. The calculated results for relaxed (a) 1,5- and (b) 2,6-DBAQ structures from a first-principle study based on density functional theory. A square and a parallelogram with two unit cell vectors are unit cells in (a) and (b), respectively. Sixteen possible intermolecular interactions are drawn with dotted lines for a molecule in unit cells. The energy gains per molecule as a function of lattice parameters for (c) 1,5- and (d) 2,6-DBAQ, respectively. Circles, triangles and squares are the results of the calculations, and the curves represent fittings. For 2,6-DBAQ, only two graphs are selected to display for simplicity with the fixed angle and ratio between a and b, although we performed calculations considering them as each independent variable.

four possible bonds: two O···H bonds, a Br···H bond, and a Br···Br bond, as depicted with dotted lines in Figure 3(c). The halogen bond between two Br atoms is evidenced by the angular orientation of the molecules; namely, the positive potential region of a Br atom points toward the negative part of the other Br atom. The direction of the Br···H bond is also determined by the negative potential region of a Br atom. These two Br···Br and Br···H bonds form a triangular structure, making an acute angle around a Br atom. Such acute-triangular structures were found in various supramolecular structures such as molecular chains, ladders, and layered structures.[14−16] Due to their structural rigidity, it has been suggested that they could be used in the construction of molecular nanobaskets for drug delivery applications.[16] We note that an H atom forms a similar triangular structure with Br···H and O···H bonds, and that an O atom does so with two O···H bonds.

The chevron structures of 2,6-DBAQ consist of two alternating molecular rows. Each row consists of equally spaced parallel molecules. Along a row, two neighboring molecules have four possible bonds: two O···Br and two Br···H bonds, as depicted with black dotted lines in Figure 3(d). The observation of O···Br bonds *in our direct method* confirms the existence of a positive potential region in a Br atom. When O···Br bonds were first observed in the chains of alternating 1,4-dioxane and Br$_2$ molecules by Hassel in the early 1950s, the relevance of such bonds was debatable due to their small electronegativity difference.[1] In Figure 3(d), six bonds are drawn across rows. When the number of bonds is correctly counted, there will be four possible bonds per molecule across rows: two O···H and two Br···H bonds, as depicted in the figure with red dotted lines (also in Figure 4(b)). Similar to the 1,5-DBAQ case, there are

several triangular structures in the 2,6-DBAQ system. A Br atom simultaneously forms an O···Br bond and two Br···H bonds, making two different triangles that share an O···Br bond. O atoms also form two simultaneous bonds, O···Br and O···H, which make an almost orthogonal angle around an O atom. In the protein structures of α-helices and β-sheets, O···Br and O···H bonds form orthogonal triangles around an O atom, similar to the 2,6-DBAQ case.[12] In the orthogonal structures, two bonds are independent in both the geometric and energetic senses, such that one bond can be easily added or removed without significantly perturbing the other bond during protein folding reactions.[12]

To understand the precise arrangement of 1,5- and 2,6-DBAQ molecules, we performed a first-principles calculation based on density functional theory. The calculation results, shown in Figure 4, parts (a) and (b), clearly reproduced our models. In the 1,5-DBAQ molecules, the two unit cell vectors formed a square. The long axes of two neighboring 1,5-DBAQ molecules made a 90° angle, and the equilibrium lattice distance, the magnitude of the unit cell vectors was 1.40 nm, consistent with experimental observations (89.5° ± 0.5° and 1.41 ± 0.05 nm). In the 2,6-DBAQ molecules, the two unit cell vectors formed a rectangle, and the long axes of two neighboring 2,6-DBAQ molecules across the rows made an 85° angle. The equilibrium lattice distances along two orthogonal directions were 1.75 and 1.03 nm. They both show reasonable agreement with experimental observations (84.5° ± 0.5°, 1.76 ± 0.05 nm and 0.98 ± 0.05 nm).

Since the characteristic features of our models are in good agreement with the calculation results, quantitative bond distances and angles were extracted from the calculation results as

2299

dx.doi.org/10.1021/jp110891y |*J. Phys. Chem. C* 2011, 115, 2297–2301

Figure 5. (a) Schematic defining the intermolecular bond distance, angle θ_1 around an electrophillic atom and angle θ_2 around a nucleophilic atom. (b) Measured bond distances for four intermolecular bonds (squares) in 1,5- and 2,6-DBAQ structures and their sum of the van der Waals radii (dotted lines) in references. (c) Measured θ_1 (circles) and θ_2 (triangles) for four intermolecular bonds in 1,5- and 2,6-DBAQ structures and their medians (dotted lines) in references.

summarized in Figure 5. As references, the distances were compared with sum of the van der Waals radii of two bonded atoms, and the angles were displayed together with the medians of angles from previous reports.[34−42] Since a typical width of intermolecular potential is 0.1 nm, the bond distances of four different kinds of intermolecular bonds in the 1,5- and 2,6-DBAQ structures are quite close to the reported sum of the van der Waals radii as shown in Figure 5(b). This confirms that these four bonds are real entities of our molecular structures. An O···H bond has a distance of 0.31 nm which is 0.05 nm longer than sum of the van der Waals radii, thereby implying that this is a weak hydrogen bond.[35]

In Figure 5(a), angles θ_1 and θ_2 are defined for each bond. The values of θ_1 around electrophillic atoms (Br and H) tend to be close to 180°, consistent with reported medians.[35−39] This is explained by the distribution of electrostatic potentials at H and Br atoms.[1−4,38] Even though their origins and the overall distributions are different, both Br and H atoms have the highest positive electrostatic potential around 180°.[1−4,38] In the O···H bonds, two θ_1 angles appear to deviate from the reported median as a result of competition against other stronger bonds.[38] Around nucleophilic atoms (Br and O), the θ_2 angles were observed between 90° and 135°.[38−42] In the Br···H and Br···Br bonds, the θ_2 angles in DBAQ systems are in good agreement with the reported medians, 100° and 90°, respectively, and are also explained by the potential distribution at Br atoms.[39−41] Around O atoms, the reported median of 120° originated from the distribution of two lone pair electrons in three-dimensional systems.[38] The observed θ_2 angles in our systems are consistently larger than 120°, which implies that lone pair electrons participated in adsorption binding to the substrate, leaving behind the modified charge distribution in O atoms.

The net energy gains for the structures of 1,5- and 2,6-DBAQ molecules are 208 and 184 meV per molecule, respectively, as shown in Figure 4, parts (c) and (d). (The results by the hybrid functional method (B3LYP) are 329 meV, and 288 meV, respectively.[27−30]) In previous bulk experiments and calculations, the strengths (distances) of O···H, Br···H, Br···Br,

and Br···O bonds under similar molecular environments (covalently bonded to C atoms) were about 50 meV (0.28 nm), 70 meV (0.30 nm), 60 meV (0.38 nm), and 60 meV (0.38 nm), respectively.[43−48] On the basis of these bond strengths, the energy gains of the systems can be estimated by counting the number of intermolecular bonds per molecule. A 1,5-DBAQ molecule has 2 O···H, 4 Br···H, and 2 Br···Br bonds, whereas a 2,6-DBAQ molecule has 2 O···H, 4 Br···H, and 2 O···Br bonds, as shown in Figure 4, parts (a) and (b). Therefore, the expected energy gains for both structures are 500 meV per molecule. The above computational results are significantly lower than this rough estimation. Some part of the discrepancy may be related to the weakness of density functional theory such as the inability to describe the dispersion interactions. In fact, the application of semiempirical van der Waals interactions increased the binding energies to 440 and 471 meV for 1,5-DBAQ and 2,6-DBAQ molecules.[31]

5. CONCLUSIONS

In conclusion, we studied the supramolecular structures of 1,5- and 2,6-DBAQ on Au(111) using STM. In both systems, we observed triangular structures including Br···Br or O···Br halogen bonds. On the basis of STM images, we propose molecular models that were well-reproduced by first-principles studies and are explained in the context of halogen and hydrogen bonds. Measured bond distances, angles, and strengths are consistent with existing bulk data. Our work directly visualizes the cooperation of two different kinds of intermolecular interactions. The observed triangular structures can be used to create robust supramolecular structures in various dimensions.

■ ASSOCIATED CONTENT

ⓢ Supporting Information. Additional experimental results on Bias-dependent STM images of 1,5-DBAQ network and 2,6-DBAQ network. This material is available free of charge via the Internet at http://pubs.acs.org.

■ AUTHOR INFORMATION

Corresponding Author
*Tel: (+82) 2-3290-3109; Fax: (+82) 2-922-3484; E-mail: sjkahng@korea.ac.kr.

■ ACKNOWLEDGMENT

■ REFERENCES

(1) Hassel, O. *Science* **1970**, *170*, 497.
(2) Metrangolo, P.; Resnati, G.; Arman, H. D., *Halogen Bonding: Fundamentals and Applications*, Springer-Verlag, Berlin, 2008.
(3) Desiraju, G. R.; Parthasarathy, R. *J. Am. Chem. Soc.* **1989**, *111*, 8725.
(4) Metrangolo, P.; Meyer, F.; Pilati, T.; Resnati, G.; Terraneo, G. *Angew. Chem., Int. Ed.* **2008**, *47*, 6114.
(5) Hernandes, M. Z.; Cavalcanti, S. M. T.; Moreira, D. R. M.; de Azevedo, W. F.; Leite, A. C. L. *Curr. Drug Targets* **2010**, *11*, 303.

(6) Leite, A. C. L.; Moreira, D. R. M.; Cardoso, M. V. O.; Hernandes, M. Z.; Pereira, V. R. A.; Silva, R. O.; Kiperstok, A. C.; Lima, M. S.; Soares, M. B. P. *ChemMedChem* **2007**, *2*, 1339.

(7) Gerebtzoff, G.; Li-Blatter, X.; Fischer, X. H.; Frentzel, A.; Seelig, A. *ChemBioChem* **2004**, *5*, 676.

(8) Acharya, C.; Seo, P. R.; Polli, J. E.; MacKerell, A. D. *Mol. Pharm.* **2008**, *5*, 818.

(9) Jeschke, P. *Pest Manage. Sci.* **2010**, *66*, 10.

(10) Lu, Y.; Shi, T.; Wang, Y.; Yang, H.; Yan, X.; Luo, X.; Jiang, H.; Zhu, W. *J. Med. Chem.* **2009**, *52*, 2854.

(11) Voth, A. R.; Hays, H. A.; Ho, P. S. *Proc. Natl. Acad. Sci. U.S.A.* **2007**, *104*, 6188.

(12) Voth, A. R.; Khuu, P.; Oishi, K.; Ho, P. S. *Nat. Chem.* **2009** *1*, 74.

(13) Metrangolo, P.; Resnati, G. *Science* **2008**, *321*, 918.

(14) Navon, O.; Bernstein, J.; Khodorkovsky, V. *Angew. Chem., Int. Ed.* **1997**, *36*, 601.

(15) Lieberman, H. F.; Davey, R. J.; Newsham, D. M. T. *Chem. Mater.* **2000**, *12*, 490.

(16) Gibb, C. L. D.; Stevens, E. D.; Gibb, B. C. *J. Am. Chem. Soc.* **2001**, *123*, 5849.

(17) Corradi, E.; Meille, S. V.; Messina, M. T.; Metrangolo, P.; Resnati, G. *Angew. Chem., Int. Ed.* **2000**, *39*, 1782.

(18) Saha, B. K.; Nangia, A.; Jaskólski, M. *CrystEngComm* **2005** *7*, 355.

(19) Sun, A.; Lauher, J. W.; Goroff, N. S. *Science* **2006**, *312*, 1030.

(20) Aakeröy, C. B.; Fasulo, M.; Schultheiss, N.; Desper, J.; Moore, C. *J. Am. Chem. Soc.* **2007**, *129*, 13772.

(21) Aakeröy, C. B.; Desper, J.; Helfrich, B. A.; Metrangolo, P.; Pilati, T.; Resnati, G.; Stevenazzi, A. *Chem. Commun.* **2007**, 4236.

(22) Politzer, P.; Murray, J. S.; Lane, P. *Int. J. Quantum Chem.* **2007**, *107*, 3046.

(23) Kresse, G.; Hafner., J. *Phys. Rev. B.* **1993**, *47*, 558.

(24) Kresse, G.; Hafner., J. *Phys. Rev. B.* **1994**, *49*, 14251.

(25) Blöchl, P. E. *Phys. Rev.B.* **1994**, *50*, 17953.

(26) Perdew, J. P.; Burke, K.; Ernzerhof, M. *Phys. Rev. Lett.* **1996** *77*, 3865.

(27) Vosko, S. H.; Wilk, L.; Nusair, M. *Can. J. Phys.* **1980**, *58*, 1200.

(28) Lee, C.; Yang, W.; Parr, R. G. *Phys. Rev. B* **1988**, *37*, 785.

(29) Becke, A. D. *J. Chem. Phys.* **1993**, *98*, 5648.

(30) Stephens, P. J.; Devlin, F. J.; Chabalowski, C. F.; Frisch, M. J. *J. Phys. Chem.* **1994**, *98*, 11623.

(31) Grimme, S. *J. Comput. Chem.* **2004**, *25*, 1463.

(32) Elemans, J. A. A. W.; Lei, S.; De Feyter, S. S. *Angew. Chem., Int. Ed.* **2009**, *48*, 7298.

(33) Xu, W.; Kelly, R. E. A.; Gersen, H.; Laegsgaard, E.; Stensgaard, I.; Kantorovich, L. N.; Besenbacher, F. *Small* **2009**, *5*, 1952.

(34) Rowland, R. S.; Taylor, R. *J. Phys. Chem.* **1996**, *100*, 7384.

(35) Desiraju, G. R.; Steiner, T., *The Weak Hydrogen Bond in Structural Chemistry and Biology*; Oxford University Press: Oxford/ New York, 1999.

(36) Rajnikant, V.; Jasrotia, D.; Chand, B. *J. Chem. Crystallogr.* **2008**, *38*, 211.

(37) Neve, F.; Crispini, A. *Cryst. Growth Des.* **2001**, *1*, 387.

(38) Steiner, T. *Angew. Chem., Int. Ed.* **2002**, *41*, 48.

(39) Ramasubbu, N.; Parthasarathy, R.; Murray—Rust, P. *J. Am. Chem. Soc.* **1986**, *108*, 4308.

(40) Auffinger, P.; Hays, F. A.; Westhof, E.; Ho, P. S. *Proc. Natl. Acad. Sci. U.S.A.* **2004**, *101*, 16789.

(41) Brammer, L.; Bruton, E. A.; Sherwood, P. *Cryst. Growth Des.* **2001**, *1*, 277.

(42) Lommerse, J. P. M.; Stone, A. J.; Taylor, R.; Allen, F. H. *J. Am. Chem. Soc.* **1996**, *118*, 3108.

(43) Pawin, G.; Solanki, U.; Kwon, K. -Y.; Wong, K. L.; Lin, X.; Jiao, T.; Bartels, L. *J. Am. Chem. Soc.* **2007**, *129*, 12056.

(44) Futami, Y.; Kudoh, S.; Ito, F.; Nakanaga, T.; Nakata, M. *J. Mol. Struct.* **2004**, *690*, 9.

(45) Kovács, A.; Varga, Z. *Coord. Chem. Rev.* **2006**, *250*, 710.

(46) Xu, J.; Wang, W.-L.; Lin, T.; Sun, Z.; Lai, Y.-H. *Supramol. Chem.* **2008**, *20*, 723.

(47) Awwadi, F. F.; Willett, R. D.; Peterson, K. A.; Twamley, B. *Chem.—Eur. J.* **2006**, *12*, 8952.

(48) Riley, K. E.; Murray, J. S.; Politzer, P.; Concha, M. C.; Hobza, P. *J. Chem. Theory Comput.* **2009**, *5*, 155.

2301

dx.doi.org/10.1021/jp110891y |*J. Phys. Chem. C* 2011, 115, 2297–2301